The Thermodynamic Control of Tropical Rainfall*

David J. Raymond
Physics Department and Geophysical Research Center
New Mexico Tech
Socorro, NM 87801 USA
raymond@kestrel.nmt.edu

May 16, 2006

Abstract

Neelin and Held (1987) showed how surface heat fluxes and infrared radiation control atmospheric convergence in the tropics, and hence rainfall there, via their joint effect on the supply of moist static energy to the troposphere. They also showed that for a given rate of supply of moist static energy, the strength of convergence is inversely proportional to a "gross moist stability", which is related to the humidity of the troposphere and to the difference between the height of the environmental minimum in moist static energy and the elevation of maximum vertical mass flux. This paper extends Neelin and Held's analysis to the non-equilibrium case by invoking the somewhat speculative hypothesis that rainfall is primarily controlled by the mean saturation deficit of the troposphere. The relaxation time of the atmosphere to the Neelin-Held equilibrium is found to be a strong function of the existing saturation deficit under this hypothesis.

Contents

1 Introduction **2**

2 Non-equilibrium model **4**

3 Model solutions **7**

3.1 Steady solutions 7

3.2 Behavior near steady solutions 7

3.3 Full solution 8

*In press, Quart. J. Roy. Meteor. Soc.

4 Discussion **9**
4.1 Vertical velocity and precipitation 10
4.2 Feedbacks 10
4.3 Role of convective dynamics 11
4.4 Quasi-equilibrium theories 11
4.5 Mechanical versus thermodynamic forcing 12

5 Further work **12**

6 References **12**

1 Introduction

The means by which the large scale atmospheric circulation controls convection and precipitation is still a matter of controversy. Here we attempt to illuminate this matter by extending the ideas of Neelin and Held (1987; hereafter NH87). NH87 related the change in the moist static energy of air passing through convective systems to the net input of energy into the troposphere by surface fluxes and radiation. This allowed NH87 to infer how horizontal divergence is related to radiative and surface heat flux forcing. However, their analysis is only useful in the steady state. The purpose of this paper is to extend the analysis to the non-equilibrium case.

The quantities moist static energy and moist entropy have quite similar properties in the atmosphere — the main difference is that the former is approximately conserved between hypothetical static states with zero kinetic energy before and after a dynamic event, while the latter is conserved during dynamic events to the extent that they operate in reversible adiabatic fashion. Neither is perfectly conserved between real atmospheric states, so the choice of which to use is somewhat a matter of taste. In this paper we recast the arguments of NH87 in terms of entropy and the closely related quantity equivalent potential temperature.

Figure 1 illustrates the entropy currents pertinent to the analysis of NH87. In a steady situation NH87 note that

$$I_{es} - I_{ed} = I_{eout} - I_{ein}. \tag{1}$$

In other words, the import of entropy (or moist static energy) into the control volume of figure 1 by surface convective and radiative fluxes, I_{es}, minus the net radiative loss of entropy to outer space, I_{ed}, equals the net export of entropy by lateral mass currents, $I_{eout} - I_{ein}$.[1] However, we can write $I_{eout} - I_{ein} = M\delta s_m$, where M is the rate at which mass passes through the control volume and δs_m is the difference between the mass-weighted means of moist entropy entering and leaving the box. Solving for M, we find

[1] We ignore here the production of entropy in the box, which must be considered in a full accounting. Entropy production is formally included in the next section.

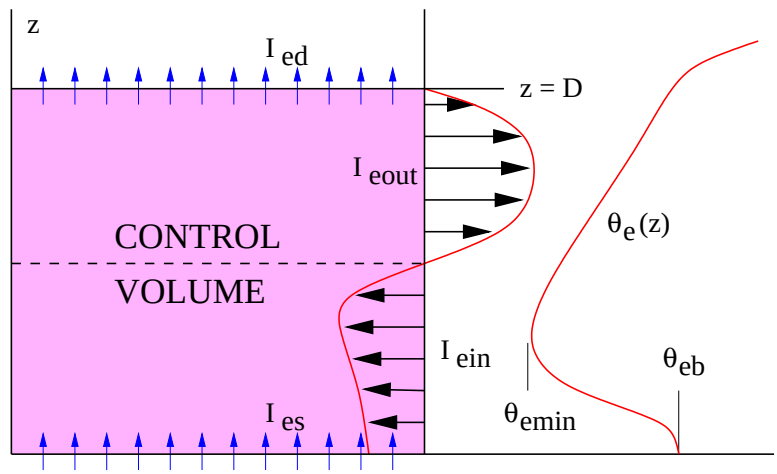

Figure 1: Illustration of entropy currents pertinent to the analysis of NH87. The control volume is a region of the troposphere, defined by the shaded box with top at the tropopause $z = D$. Note that the profile of θ_e is that of the environment outside the control volume in this case. The dashed line indicates the level of convective non-divergence.

that

$$M = \frac{I_{es} - I_{ed}}{\delta s_m}. \tag{2}$$

Thus, for a given $I_{es} - I_{ed}$, the mass current M through the box and hence the net upward mass current through the level of non-divergence is inversely proportional to δs_m. This quantity in turn is likely to scale with the difference between surface and minimum values of equivalent potential temperature in the environmental sounding, $\theta_{eb} - \theta_{emin}$. Therefore, the smaller $\theta_{eb} - \theta_{emin}$, the larger M. Moist environments with near-neutral stability, and hence smaller $\theta_{eb} - \theta_{emin}$, more readily respond to net entropy forcing, $I_{es} - I_{ed}$. Such environments are characterized by NH87 as having small *gross moist stability*.

Note that for positive gross moist stability, the minimum in the environmental θ_e profile generally occurs at an elevation lower than that of the level of non-divergence for convection, as illustrated in figure 1. This way the inflow into convection has smaller average values of θ_e than the outflow.[2]

On day-to-day time scales, the steady state assumption inherent in the analysis of NH87 cannot obviously be justified. However, the introduction of additional information bolsters the analysis. Recent observational (Raymond and Wilkening, 1985; Brown and Zhang, 1997; DeMott and Rutledge, 1998) and numerical work (Tompkins and Craig, 1998; Raymond and Torres, 1998) suggests that the precipitation produced by convection is a strong function of the relative humidity of the atmosphere, with higher humidities

[2]One can imagine pathological cases where this relationship does not hold, but they tend not to occur in real soundings.

resulting in stronger precipitation. The main reason for this is the sensitivity of convection to entrainment by environmental air — the moister this air, the less tendency there is for it to evaporate condensed water in the updraft, thereby reducing both liquid water content and updraft buoyancy.

NH87 are silent on the possibility that the gross moist stability might be negative. However, this would appear to be a very unlikely eventuality, since it would be subject to spontaneous blowups in which precipitation results in the *import* of moist static energy from the environment into the precipitating region, which results in heavier precipitation, etc. We will ignore this possibility.

In this paper we introduce a rather extreme working hypothesis, namely that the precipitation rate over tropical oceans depends *only* on the mean saturation deficit of the troposphere. This hypothesis plus some other relatively minor assumptions allow the moist entropy budget of the troposphere to be closed in the non-steady case, resulting in a model for the evolution of precipitation rate and tropospheric humidity over the tropical oceans.

The above hypothesis may be viewed as being outrageously oversimplified, and only a small amount of quantitative evidence exists to support it at this point. However, Raymond and Torres (1998) found in an analysis of numerical simulations of the tropics that rainfall rate correlated more closely with the saturation deficit than with any other plausible variable, far exceeding the correlation with surface convergence or sea-air heat flux. Given its simplicity and plausibility, it seems worth exploring the consequences of the above hypothesis.

2 Non-equilibrium model

The governing equations for equivalent potential temperature θ_e and total water mixing ratio r_t (vapor plus cloud droplets plus small ice crystals) are

$$\frac{\partial \rho\theta_e}{\partial t} + \nabla \cdot (\rho \mathbf{u}\theta_e) + \frac{\partial \rho w\theta_e}{\partial z} = -\frac{\partial F_e}{\partial z} + G \tag{3}$$

and

$$\frac{\partial \rho r_t}{\partial t} + \nabla \cdot (\rho \mathbf{u} r_t) + \frac{\partial \rho w r_t}{\partial z} = -\frac{\partial F_r}{\partial z} - P \tag{4}$$

where $\rho(z)$ is the air density, $\mathbf{u}$ and w are the horizontal and vertical wind components (with convective fluctuations smoothed out), F_e is the vertical equivalent potential temperature flux from turbulence, convection, and radiation, G is related to the generation of entropy by irreversible processes, F_r is the vertical flux of total cloud water, and P is the net conversion rate of total cloud water to and from precipitation.

In the tropics the temperature profile of the atmosphere doesn't change much with time, due to the tendency of gravity waves to laterally redistribute buoyancy anomalies. Thus, the saturated equivalent potential temperature θ_{es} and the saturation mixing

ratio r_s are essentially functions of height alone. This fact allows us to recast the above equations into a more useful form.

Let us define the equivalent potential temperature deficit $\Delta\theta_e = \theta_{es} - \theta_e$ and the saturation deficit $\Delta r = r_s - r_t$.[3] For a fixed temperature profile,

$$\Delta\theta_e \approx \theta_{es} L \Delta r/(C_p T_R), \tag{5}$$

where C_p is the specific heat at constant pressure, L is the latent heat of condensation, and T_R is a constant reference temperature. Thus, the two quantities $\Delta\theta_e$ and Δr are proportional to each other, with the proportionality factor being a function only of height.

Let us now average (3) and (4) over a control volume of area A and depth D, indicating this average by an overbar. Assuming that $w = 0$ both at the surface and at $z = D$, the top of the control volume, we find

$$-\frac{d\overline{\rho\Delta\theta_e}}{dt} + \frac{M\delta\theta_e}{AD} = \frac{F_{es} - F_{ed}}{D} + \overline{G} \tag{6}$$

and

$$-\frac{d\overline{\rho\Delta r}}{dt} - \frac{M\delta r_t}{AD} = \frac{F_{rs} - R}{D}. \tag{7}$$

The areally averaged total (convective plus radiative) equivalent potential temperature fluxes at the surface and at $z = D$ are respectively F_{es} and F_{ed}, F_{rs} is the areally averaged surface evaporation rate, and $R = D\overline{P}$ is the areally averaged rainfall rate.

The control volume average of the horizontal equivalent potential temperature flux divergence is obtained as follows:

$$\begin{aligned} \frac{1}{AD}\int_0^d \int_A \nabla\cdot(\rho\mathbf{u}\theta_e)dAdz &= \frac{1}{AD}\int_0^d dz \oint \rho\theta_e \mathbf{u}\cdot\mathbf{n}ds \\ = \frac{-M\theta_{ein} + M\theta_{eout}}{AD} &\equiv \frac{M\delta\theta_e}{AD}, \end{aligned} \tag{8}$$

where the line integral in the second term is around the periphery of the control volume, $\mathbf{n}$ is a horizontal outward unit normal to the control volume, M is the mass current through the control volume, θ_{ein} and θ_{eout} are the weighted averages of equivalent potential temperature flowing into and out of the control volume sides, where the weighting factor in each case is $\rho\mathbf{u}\cdot\mathbf{n}$, and $\delta\theta_e$ is the difference between these averages. A similar analysis of the total cloud water yields

$$\frac{1}{AD}\int_0^D \int_A \nabla\cdot(\rho\mathbf{u}r_t)dAdz = \frac{-Mr_{tin} + Mr_{tout}}{AD} \equiv -\frac{M\delta r_t}{AD}, \tag{9}$$

where the minus sign in the definition of δr_t is imposed because generally $r_{tout} < r_{tin}$. Thus, $\delta\theta_e = \theta_{eout} - \theta_{ein}$, while $\delta r_t = r_{tin} - r_{tout}$.

[3] For Δr truly to be the saturation deficit, r_t should be replaced by the vapor mixing ratio. However, to the extent that conversion of cloud water to precipitation is efficient, the error should be small.

Using (5), it is possible to eliminate the time derivatives between (6) and (7) resulting in an equation for the mass current M:

$$M = A\frac{F_{es} - F_{ed} + D\overline{G} + \theta_{es}L(R - F_{rs})/(C_pT_R)}{\delta\theta_e + \theta_{es}L\delta r_t/(C_pT_R)}. \tag{10}$$

Thus, the mass current in this model is a function of the entropy fluxes at the surface and the tropopause, the irreversible generation of entropy, and rainfall minus evaporation. Note that this result is not limited to steady situations. It therefore constitutes an extension of the results of NH87 to the non-steady case.

Furthermore, eliminating M between (6) and (7) yields

$$-\frac{d\chi}{dt} = -\frac{(R - F_{rs})\delta\theta_e}{D\delta r_t} + \frac{F_{es} - F_{ed}}{D} + \overline{G}. \tag{11}$$

where

$$\chi = \overline{\rho\Delta\theta_e} + \frac{\overline{\rho\Delta r}\delta\theta_e}{\delta r_t} \approx \left(\frac{\overline{\theta_{es}}L}{C_pT_R} + \frac{\delta\theta_e}{\delta r_t}\right)\overline{\rho\Delta r}. \tag{12}$$

The last step assumes that $\overline{\theta_{es}\rho\Delta r} \approx \overline{\theta_{es}}\,\overline{\rho\Delta r}$. Thus, χ is essentially proportional to Δr, and is therefore large for a dry atmosphere and small for a moist atmosphere.

We now explore the consequences of linking the rainfall rate to the saturation deficit. One can express the hypothesis that rainfall is a function of the mean saturation deficit in the convective region by assuming that $R = R(\chi)$. Let us give this a definite form with the assumption that

$$R = \frac{R_0\chi_0}{\chi}, \tag{13}$$

where R_0 is the rainfall rate under a reference condition, which we take to be that associated with radiative-convective equilibrium. Further, the constant χ_0 is the value of χ occurring under these conditions. The inverse dependence on χ means that the rainfall rate becomes infinite if the atmosphere becomes perfectly saturated. The radiative-convective equilibrium precipitation rate in the tropics is about 4 mm day^{-1} $\approx 5 \times 10^{-5}$ kg m^{-2} s^{-1}. A plausible value for χ_0 is ≈ 5 kg K m^{-3}.

The time derivative of χ can be related to the time derivative of R using the above condition:

$$\frac{dR}{dt} = \frac{dR}{d\chi}\frac{d\chi}{dt} = -\frac{R_0\chi_0}{\chi^2}\frac{d\chi}{dt} = -\frac{R^2}{R_0\chi_0}\frac{d\chi}{dt}. \tag{14}$$

Eliminating the χ time derivative in (11) with this equation results in

$$\frac{R_0\chi_0}{R^2}\frac{dR}{dt} = -\frac{R\delta\theta_e}{D\delta r_t} + \frac{F_{rs}\delta\theta_e}{D\delta r_t} + \frac{F_{es} - F_{ed}}{D} + \overline{G}. \tag{15}$$

This is a prognostic equation for rainfall rate which reduces to something analogous to the steady state condition of NH87 when the time derivative is zero.

Let us nondimensionalize the above equation by defining the dimensionless rainfall rate $\alpha = R/R_0$ and the dimensionless time $\tau = t/t_0$:

$$\frac{d\alpha}{d\tau} = -\alpha^3 + \alpha^2 \Delta\phi \tag{16}$$

when we set

$$t_0 = \frac{D\chi_0 \delta r_t}{R_0 \delta\theta_e} \tag{17}$$

and define

$$\Delta\phi = \frac{F_{rs}}{R_0} + \frac{F_{es} - F_{ed} + D\overline{G}}{F_{en}} \tag{18}$$

where $F_{en} = R_0 \delta\theta_e / \delta r_t$. If we take $D = 15$ km, $\chi_0 = 5$ K kg m^{-3}, $\delta r_t = 10$ g kg^{-1}, $\delta\theta_e = 5$ K, and $R_0 = 5 \times 10^{-5}$ kg m^{-2} s^{-1}, then $t_0 = 3 \times 10^6$ s ≈ 35 d and $F_{en} = 0.025$ kg m^{-2} s^{-1} K. Converted to heat flux terms, this value is equivalent to about 25 W m^{-2}. The quantity $\Delta\phi$ is a dimensionless measure of the forcing of rainfall.

3 Model solutions

We begin with an examination of the steady state solutions of (16), followed with an analysis of the stability of these solutions. We then solve (16) exactly for a range of values of the forcing parameter $\Delta\phi$.

3.1 Steady solutions

If we set the time derivative to zero in (16), we readily find that $\alpha = 0$ and $\alpha = \Delta\phi$ satisfy the equation. These correspond physically to the case of no rain and to the case of steady rain at a rate equal to $\Delta\phi$ times the radiative-convective equilibrium rainfall rate. The latter solution is only physically meaningful when $\Delta\phi \geq 0$. Let us call it the equilibrium solution $\alpha_{eq} \equiv \Delta\phi$.

3.2 Behavior near steady solutions

If we set $\alpha = \Delta\phi + \alpha'$, substitute into (16), and linearize in terms of α', we find that

$$\frac{d\alpha'}{d\tau} = -\Delta\phi^2 \alpha'. \tag{19}$$

This has the solution

$$\alpha' \propto \exp(-\Delta\phi^2 \tau), \tag{20}$$

which means that the equilibrium solution is stable, with perturbations decaying on a dimensionless time scale of $1/\Delta\phi^2$. Thus, the stronger the forcing, the shorter the decay transient.

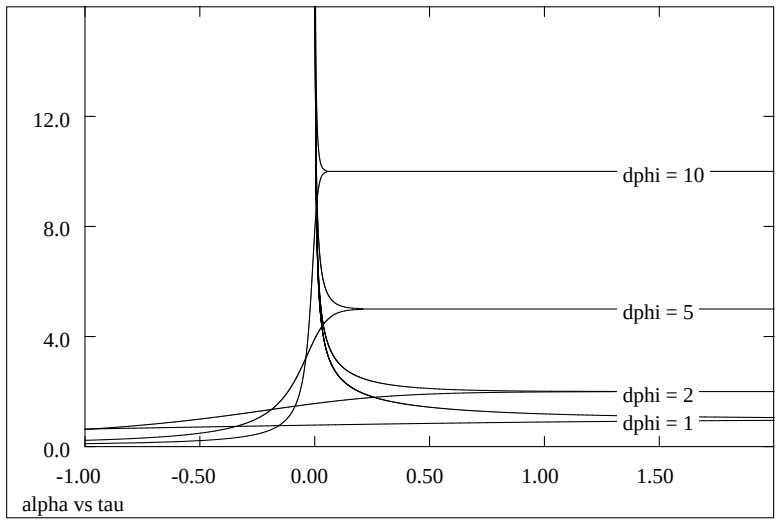

Figure 2: Full solution to the equation for dimensionless precipitation rate α as a function of dimensionless time τ. Solutions starting both above and below the equilibrium precipitation rate are shown for $\Delta\phi = 1, 2, 5, 10$.

No linearization is possible about the solution at $\alpha = 0$ — the solution is inherently nonlinear. However, where $|\alpha| \ll |\Delta\phi|$ we have the approximate governing equation

$$\frac{d\alpha}{d\tau} = \alpha^2 \Delta\phi, \tag{21}$$

which has the solution

$$\alpha = [\Delta\phi(\tau_0 - \tau)]^{-1}, \tag{22}$$

where τ_0 is a constant of integration. Note that for positive $\Delta\phi$, the solution has α asymptotically approaching infinity as $\tau \to \tau_0$. This limit violates the initial approximation, but it does show that the $\alpha = 0$ solution is unstable for positive forcing. On the other hand, if $\Delta\phi < 0$, α decays to zero as τ increases, which means that the steady solution is stable in that case.

In summary, if $\Delta\phi$ is positive, α tends toward $\alpha_{eq} = \Delta\phi$, with the tendency being more rapid if $\Delta\phi$ is large. If $\Delta\phi < 0$, α tends toward zero.

3.3 Full solution

Equation (16) has an exact solution, which however can only be expressed explicitly as $\tau = \tau(\alpha)$ rather than vice versa:

$$\tau = \tau_0 + \frac{1}{\Delta\phi^2} \ln\left(\frac{\alpha}{|\Delta\phi - \alpha|}\right) - \frac{1}{\Delta\phi\alpha}. \tag{23}$$

The quantity τ_0 is again a constant of integration. This solution is plotted in figure 2 for $\tau_0 = 0$ and for four different values of $\Delta\phi$.

These results confirm the earlier assertion that $\alpha = 0$ is an unstable solution while $\alpha = \alpha_{eq} = \Delta\phi$ is stable for $\Delta\phi > 0$. They also illustrate how dramatically the transient time decreases as $\Delta\phi$ increases, further confirming the results of the linearized analysis.

4 Discussion

The results presented here are based on the following hypotheses:

- The precipitation rate is a unique decreasing function of the mean saturation deficit of the convective environment.
- The temperature profile of the convective environment doesn't change with time.

Based on these hypotheses, we find the following:

- The rainfall rate tends to relax toward an equilibrium value equal to

$$R_{eq} = \alpha_{eq} R_0 = \Delta\phi R_0 = F_{rs} + \frac{\delta r_t (F_{es} - F_{ed} + D\overline{G})}{\delta\theta_e}. \tag{24}$$

  Thus, in equilibrium, the excess or deficit of precipitation relative to the surface evaporation rate depends on the sign of $F_{es} - F_{ed} + d\overline{G}$. However, its strength depends as well on δr_t and $\delta\theta_e$. The parameter δr_t doesn't vary much since the mixing ratio typically drops off rapidly with height, so that δr_t is approximately equal to the mean value of the total water mixing ratio below the convective level of non-divergence. However, $\delta\theta_e$ depends sensitively on the relative heights of the level of non-divergence and the minimum in environmental θ_e — when the two are of comparable height, $\delta\theta_e$ will be small, whereas $\delta\theta_e$ will be larger if the level of non-divergence is much higher than the level of minimum θ_e. Negative $\delta\theta_e$ is unlikely to occur in the real atmosphere, as this represents a highly unstable situation under the present hypotheses.

- Small deviations from this equilibrium state relax on the time scale $t_0/(\Delta\phi^2)$. Since $\Delta\phi$ can vary widely, the relaxation time scale is also widely variable. For instance, if $\Delta\phi = 1$, corresponding to a radiative-convective equilibrium rainfall rate of ≈ 4 mm d^{-1}, the relaxation time is ≈ 35 d according to the estimate made in the last section. However, in a rainy region with $\alpha_{eq} = \Delta\phi = 6$, corresponding to a rainfall rate of ≈ 24 mm d^{-1}, the relaxation time is about one day.

- Even when $\alpha_{eq} \gg 1$, the relaxation time can be large if the initial state is dry and therefore has a low precipitation rate. This is evident in the $\Delta\phi = 10$ case of figure 2. The precipitation rate in this case slowly increases over an extended period and then suddenly increases to the equilibrium value.

4.1 Vertical velocity and precipitation

In radiative-convective equilibrium the surface evaporation rate is precisely equal to the precipitation rate. Furthermore, the mean vertical velocity is precisely zero at all levels.

Radiative-convective equilibrium corresponds to the case in which $\Delta\phi = 1$. If $\Delta\phi > 1$, then the equilibrium mean motion in the troposphere is upward and the equilibrium rainfall rate exceeds the local evaporation rate. This is because moist air is drawn in laterally at low levels and expelled at upper levels after loosing most of its moisture.

If $0 < \Delta\phi < 1$, then mean tropospheric motion is downward and equilibrium rainfall is less than surface evaporation, even though some deep convection may exist. Air moistened by low precipitation efficiency convection is exported to other regions. If $\Delta\phi < 0$, then no precipitation occurs at all in equilibrium in this picture.

The above three regimes correspond well to Gray's (1973) categorization of the tropics into clear regions ($\Delta\phi < 0$), variably cloudy regions with little precipitation ($0 < \Delta\phi < 1$), and heavily precipitating cloud clusters ($\Delta\phi > 1$).

4.2 Feedbacks

Let us remind ourselves that unlike $\Delta\theta_e$, which is defined in the interior of the control volume and is therefore subject to local modification by the clouds there, $\delta\theta_e$ is defined on the boundary of the control volume, and is externally determined, at least to the extent that its value is a function of the equivalent potential temperature of inflowing air.[4] Thus, we normally don't consider the possibility that the control volume convection will itself modify $\delta\theta_e$ by modifying θ_e on lateral control volume boundaries. However, moistening in the interior of the control volume can change the character of the convection there, resulting in a change in the height of the level of convective non-divergence. If this change in height is downward, then the value of $\delta\theta_e$ is decreased and the rainfall rate is increased simply because the outflowing air has a smaller value of θ_e relative to that of the inflowing air (see figure 1).

As Raymond, López, and López (1998) showed, intensifying tropical cyclones exhibit precisely this sort of transformation. Thus, a nonlinear feedback of this type may be responsible for the intensification of a tropical depression into a tropical storm. This conclusion is consistent with the idea that downdrafts decrease during intensification, as postulated by Bister and Emanuel (1997).

Another feedback which may be of considerable importance is the production of extensive middle to upper tropospheric stratus clouds by strong convection. The effect of such clouds is to reduce the outgoing longwave infrared radiation (Albrecht and Cox, 1975), resulting in larger values of $F_{es} - F_{ed}$, and therefore $\Delta\phi$. The production of extensive stratus by convection at middle to upper levels can therefore result in stronger subsequent convection.

[4] At upper levels the outflow θ_e is determined primarily by the convection itself. However, the possible range of variation in θ_e at upper levels is small as long as the temperature profile is assumed to be fixed.

4.3 Role of convective dynamics

In order to close the present theory, additional information is needed about how environmental conditions affect the updraft and downdraft mass flux profiles in convection, and in particular, what determines the level of convective non-divergence. Though we strongly suspect that the humidity of the environment plays a strong role here, this relationship needs to be better quantified. Similarly, the hypothesis that the mean saturation deficit is the primary control on precipitation rate needs to be better tested. This hypothesis is almost certainly oversimplified, and a better knowledge of the controls on precipitation will lead to better modeling of rainfall rates.

4.4 Quasi-equilibrium theories

The present work is conceptually related to some of the simpler convective quasi-equilibrium theories, such as that of Betts and Miller (Betts, 1986; Betts and Miller, 1986, 1993). In this theory in particular it is assumed that there exists a reference relative humidity profile to which the atmosphere relaxes in a very short time, say, less than a day. This relaxation is effected by dropping out as precipitation any excess amount of water vapor. In this way the precipitation rate is calculated. However, in very dry conditions, net moistening is needed to bring the relative humidity to its target value, which would require negative precipitation. The Betts-Miller scheme solves this problem by turning off the deep convective parameterization and turning on a parameterization for shallow, non-precipitating convection. Thus, the precipitation rate in the Betts-Miller scheme is a decreasing function of the mean saturation deficit of the atmosphere, as in the present model.

The original quasi-equilibrium theory of Arakawa and Schubert (1974) makes no assumptions about the time scale for humidity adjustment, asserting only that the adjustment times for the effective available potential energies of an ensemble of entraining plumes are short. Thus, the Arakawa-Schubert theory doesn't conflict with the ideas presented in this paper. Any relationship between precipitation rate and environmental humidity results from the assumed precipitation model for the convective plumes.

A different type of quasi-equilibrium theory called boundary layer quasi-equilibrium (BLQ) was developed by Raymond (1995) and Emanuel (1995), in which it is postulated that the subcloud layer entropy rapidly adjusts to an equilibrium value, resulting in a tightly controlled relationship between surface entropy fluxes and the net upward transport of entropy by convection. The latter is caused primarily by the *downward* transport of low equivalent potential temperature air into the subcloud layer. The additional postulate of a deterministic relationship between updraft and downdraft mass fluxes in convection plus an estimate of the equivalent potential temperature depression in downdrafts relative to boundary layer air leads to an estimate of updraft mass fluxes near cloud base in this theory.

Downdrafts are postulated to have greater θ_e depressions in BLQ, and to be more abundant relative to updrafts when the middle troposphere is drier. Thus, a drier middle

troposphere must result in less updraft mass flux for a given surface entropy flux. This result is similar to the conclusion reached from the present model.

4.5 Mechanical versus thermodynamic forcing

The present work postulates that precipitation in the tropics is completely controlled by thermodynamic factors. On sufficiently short time and space scales, this is clearly not true. For instance, gust fronts from earlier convection may produce convection and precipitation which wouldn't otherwise exist at that place and time, irrespective of the thermodynamic state. However, ultimately the aggregate of precipitation over a sufficiently large area and time must be consistent with thermodynamic conservation laws. The border between dynamic and thermodynamic domination of forcing is not well established at this time, and the relative importance of these two modes of convective control have yet to be determined. A significant amount of work remains to be done in this area.

5 Further work

The present work extends the ideas of Neelin and Held (1987) to the time-dependent case with the help of a somewhat speculative hypothesis about the environmental control of precipitation rate. The next step is to test this hypothesis and any alternate contenders which might be proposed. Also needed is better information about how convective updrafts and downdrafts depend on the convective environment. Both of these projects will require the development and execution of sophisticated observational and computational strategies. However, their successful resolution should result in significant progress in solving the long-standing question of what controls moist convection and precipitation in the tropical atmosphere.

Acknowledgments. The author thanks Kerry Emanuel and an anonymous reviewer for comments which greatly improved the quality of this paper. This work was supported by National Science Foundation Grant ATM-9616290 and National Oceanic and Atmospheric Administration's Pan American Climate Studies Grant GC98-632.

6 References

Albrecht, B., and S. K. Cox, 1975: The large-scale response of the tropical atmosphere to cloud modulated infrared heating. *J. Atmos. Sci.,* **32,** 16-24.

Arakawa, A., and W. H. Schubert, 1974: Interaction of a cumulus cloud ensemble with the large-scale environment, Part I. *J. Atmos. Sci.,* **31,** 674-701.

Betts, A. K., 1986: A new convective adjustment scheme. Part I: Observational and theoretical basis. *Quart. J. Roy. Meteor. Soc.,* **112,** 677-691.

Betts, A. K., and M. J. Miller, 1986: A new convective adjustment scheme. Part II: Single column tests using GATE wave, BOMEX, ATEX and arctic air-mass data sets. *Quart. J. Roy. Meteor. Soc.,* **112,** 693-709.

Betts, A. K., and M. J. Miller, 1993: The Betts-Miller scheme. *The representation of cumulus convection in numerical models.* American Meteorological Society.

Bister, M., and K. A. Emanuel, 1997: The genesis of hurricane Guillermo: TEXMEX analyses and a modeling study. *Mon. Wea. Rev.,* **125,** 2662-2682.

Brown, R. G., and C. Zhang, 1997: Variability of midtropospheric moisture and its effect on cloud-top height distribution during TOGA COARE. *J. Atmos. Sci.,* **54,** 2760-2774.

DeMott, C. A., and S. A. Rutledge, 1998: The vertical structure of TOGA COARE convection. Part II: Modulating influences and implications for diabatic heating. *J. Atmos. Sci.,* **55,** 2748-2762.

Emanuel, K. A., 1995: The behavior of a simple hurricane model using a convective scheme based on subcloud-layer entropy equilibrium. *J. Atmos. Sci.,* **52,** 3960-3968.

Gray, W. M., 1973: Cumulus, convection and larger scale circulations. Part I: Broad-scale and mesoscale considerations. *Mon. Wea. Rev.,* **101,** 839-855.

Neelin, J. D., and I. M. Held, 1987: Modeling tropical convergence based on the moist static energy budget. *Mon. Wea. Rev.,* **115,** 3-12.

Raymond, D. J., 1995: Regulation of moist convection over the west Pacific warm pool. *J. Atmos. Sci.,* **52,** 3945-3959.

Raymond, D. J., C. López-Carrillo, and L. López Cavazos, 1998: Case-studies of developing east Pacific easterly waves. *Quart. J. Roy. Meteor. Soc.,* **124,** 2005-2034.

Raymond, D. J., and D. J. Torres, 1998: Fundamental moist modes of the equatorial troposphere. *J. Atmos. Sci.,* **55,** 1771-1790.

Raymond, D. J., and M. Wilkening, 1985: Characteristics of mountain-induced thunderstorms and cumulus congestus clouds from budget measurements. *J. Atmos. Sci.,* **42,** 773-783.

Tompkins, A. M., and G. C. Craig, 1998: Radiative-convective equilibrium in a three-dimensional cloud-ensemble model. *Quart. J. Roy. Meteor. Soc.,* **124,** 2073-2097.